

Neutron emission in inelastic reactions of  $^{12}\text{C} + ^{158}\text{Gd}$  and  $^{20}\text{Ne} + ^{150}\text{Nd}$ 

G. A. Petitt

*Department of Physics and Astronomy, Georgia State University, Atlanta, Georgia 30303*

A. Gavron

*Los Alamos National Laboratory, Los Alamos, New Mexico 87545*J. R. Beene, B. Cheynis,\* R. L. Ferguson, F. E. Obenshain, F. Plasil, and G. R. Young  
*Oak Ridge National Laboratory, Oak Ridge, Tennessee 37830*

M. Jääskeläinen and D. G. Sarantites

*Department of Chemistry, Washington University, St. Louis, Missouri 63130*

C. F. Maguire

*Department of Physics, Vanderbilt University, Nashville, Tennessee 37235*

(Received 3 June 1985)

Energy spectra and angular distributions of neutrons emitted in coincidence with projectilelike fragments produced in inelastic collisions of  $^{12}\text{C}$  with  $^{158}\text{Gd}$  at 192 MeV and  $^{20}\text{Ne}$  with  $^{150}\text{Nd}$  at 176 and 239 MeV have been measured. No evidence for nonequilibrium neutron emission is found for the Ne+Nd reaction at either energy. For the C+Gd reaction a small fraction (~9%) of the neutrons emitted is due to nonequilibrium emission. The multiplicity of neutrons emitted from the targetlike fragment is, in all cases, approximately six times that of neutrons emitted from the projectilelike fragment.

## I. INTRODUCTION

Many studies of neutron emission from products of heavy ion reactions have been made over the last few years.<sup>1-21</sup> The purpose of these studies has been to detect the presence of nonequilibrium effects in the particle spectra and to compare such effects with one or more models of nonequilibrium emission. We have previously reported results on nonequilibrium neutron emission in coincidence with evaporation residues (ER) in reactions of  $^{12}\text{C}$  on  $^{158}\text{Gd}$  at bombarding energies between 110 and 192 MeV (Ref. 9) and in reactions of  $^{20}\text{Ne}$  on  $^{150}\text{Nd}$  at energies between 176 and 239 MeV.<sup>19</sup> Neutrons in coincidence with projectilelike fragments (PLF) in inelastic reactions of  $^{12}\text{C}$  on  $^{158}\text{Gd}$  have also been reported for energies up to 150 MeV.<sup>9</sup> We found evidence for nonequilibrium emission associated with both ER and PLF in all cases. The energy spectra of neutrons in coincidence with ER can be decomposed into two distinct components: a low temperature component moving with the compound nucleus velocity, and a higher temperature component which has an angular distribution consistent with evaporation from a source moving in the beam direction at a velocity intermediate between the beam and center-of-mass velocities. Moving source fits to the data show similar trends in neutron multiplicity for the Ne + Nd and C + Gd reactions with the multiplicity increasing linearly as a function of energy per nucleon above the Coulomb barrier. For a given incident bombarding energy per nucleon these effects are much more marked for the C + Gd reaction than for the Ne + Nd reaction. The threshold for nonequilibrium

emission in coincidence with ER appears to be very low for both systems, perhaps no more than 2-3 MeV/nucleon above the barrier.<sup>20,21</sup>

In contrast to the results for neutrons in coincidence with ER, no clear-cut distinction between equilibrium and nonequilibrium components could be made for neutrons in coincidence with PLF in the C + Gd reaction. However, the presence of neutron emission prior to full acceleration of the fragments was inferred from the laboratory neutron energy and angular distributions.<sup>9</sup>

Neutron energy spectra and angular distributions in coincidence with PLF have also recently been reported for several other systems.<sup>1-12</sup> The results for bombarding energies slightly above the Coulomb barrier can be explained by assuming that neutron emission takes place entirely by evaporation from the targetlike fragments (TLF) and PLF after the fragments have been fully accelerated by Coulomb repulsion following their collision.<sup>1-5</sup> Some of the results for bombarding energies well above the barrier have shown evidence for nonequilibrium emission. In addition to the results for  $^{12}\text{C} + ^{158}\text{Gd}$  discussed above, Tseruya *et al.*<sup>8,10</sup> have reported a small component of nonequilibrium neutrons for the reaction  $^{86}\text{Kr} + ^{166}\text{Er}$  at 11.9 MeV/nucleon; Gavron *et al.*<sup>7</sup> have reported a component of nonequilibrium neutrons for the reaction  $^{16}\text{O} + ^{93}\text{Nb}$  at 13 MeV/nucleon; Hilscher *et al.* found evidence for nonequilibrium emission in the reaction  $^{20}\text{Ne} + ^{165}\text{Ho}$  at energies between 11 and 20 MeV/nucleon and in the reaction  $^{12}\text{C} + ^{165}\text{Ho}$  at 25 MeV/nucleon;<sup>11</sup> and Caskey *et al.* have reported nonequilibrium emission for the reaction  $^{14}\text{N} + ^{165}\text{Ho}$  at 35 MeV/nucleon.<sup>12</sup> As in the case of non-

TABLE I. Neutron detector polar angles. (Positive angles are on the same side of the beam as the heavy ion telescope.)

Detector number	1	2	3	4	5	6	7	8	9
Angle (degrees)	-140	-65	-50	-35	-15	14	30	45	140

equilibrium emission from ER, the nonequilibrium neutron spectra are forward peaked and some of them can be parametrized in terms of emission from a moving source. However, no consistent picture of the mechanism or of the threshold for this emission has emerged.

We report here our measurements of neutron emission in coincidence with PLF in the inelastic reaction  $^{12}\text{C} + ^{158}\text{Gd}$  at 192 MeV bombarding energy and the  $^{20}\text{Ne} + ^{150}\text{Nd}$  reactions at 176 and 239 MeV. Our aim in this work was to obtain further information on nonequilibrium emission from products of inelastic reactions for the C + Gd system and to compare these results with nonequilibrium emission for the Ne + Nd system at similar bombarding energies per nucleon.

## II. EXPERIMENTAL METHOD

The experiments were performed using the Oak Ridge isochronous cyclotron. Typical beam currents were 1–2 e nA. Targets of  $^{158}\text{Gd}$  (0.85 mg/cm<sup>2</sup>) and  $^{150}\text{Nd}$  (0.9 mg/cm<sup>2</sup>) were used. Both targets were enriched to an isotopic purity greater than 96%. They were both in the form of metal foils and were stored in an inert atmosphere until ready for use. To prevent carbon or oxygen contamination of the targets during the experiment a cryopump was placed adjacent to and upstream from the target chamber. No carbon or oxygen contamination was visible on the targets when they were removed from the chamber after the experiment.

Neutron spectra were measured by the time-of-flight method with nine detectors placed at distances between 56 and 80 cm from the target. A spherical aluminum target chamber 25 cm in diameter with a wall thickness of 3 mm was used. The detectors were coplanar with the beam and with the detected PLF. Each detector consisted of an 11.25 cm diameter  $\times$  5 cm thick cell filled with NE213 liquid scintillator directly coupled to an RCA 4522 photomultiplier tube. Pulse shape discrimination was used to eliminate delayed gamma ray pulses in the neutron spectra. The temporal width of the beam bursts (which determines the resolution of the time-of-flight measurements) varied between 2.5 and 3.0 ns, depending on the beam and its energy. The effect of the time resolution on the shape of the neutron spectra was taken into account in the subsequent analysis. Heavy ion singles spectra were taken for each reaction to obtain an overall normalization with an uncertainty of approximately 30%.

The neutrons were detected in coincidence with PLF detected in a silicon  $\Delta E$ - $E$  telescope. This telescope consisted of a 300 mm<sup>2</sup>  $\times$  50  $\mu\text{m}$ -thick transmission detector backed by a 27 mm wide  $\times$  8 mm high position sensitive silicon surface barrier detector having a thickness of 500  $\mu\text{m}$ . The latter covered an angular range of 17 degrees

with the inner edge placed approximately at the grazing angle for each reaction, thus covering the laboratory angular range 13–30 degrees for the C + Gd reaction and 19–36 degrees for the Ne + Nd reaction. This arrangement enabled us to measure the single-fragment angular distribution of the PLF over the angular range of the telescope. (Knowledge of the distribution is important because it affects the forward angle distribution of neutrons emitted sequentially from the PLF.) In all cases the telescope subtended a laboratory solid angle of 27 msr.

The detector geometry and the numbering scheme used in the remainder of this paper for the neutron detectors are given in Fig. 1 and Table I. To identify high energy protons which penetrated the chamber wall, a 1 mm thick NE102A plastic scintillator detector was placed in front of each neutron detector.

Neutron detector efficiencies were determined using the data of Drog<sup>22</sup> in combination with calibration measurements with a  $^{252}\text{Cf}$  source placed at the target position. Details of the calibration procedure and the neutron-gamma discrimination scheme are given in Ref. 9. A neutron kinetic energy threshold of 2 MeV was set off line in all data analysis.

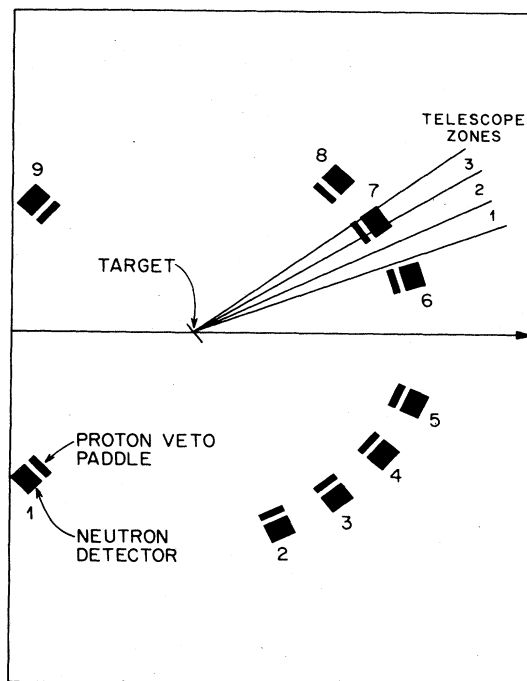


FIG. 1. Detector layout. The heavy ion detector telescope zones are shown for the position used in the Ne + Nd measurements.

## III. RESULTS

## A. Projectilelike fragment distributions

Figures 2 and 3 show typical energy distributions for PLF that were detected in the inner third of the angular range of the heavy ion telescope. This angular range, indicated as zone 1 of Fig. 1, is defined as being between 19 and 24.6 degrees for the Ne + Nd reaction and between 13

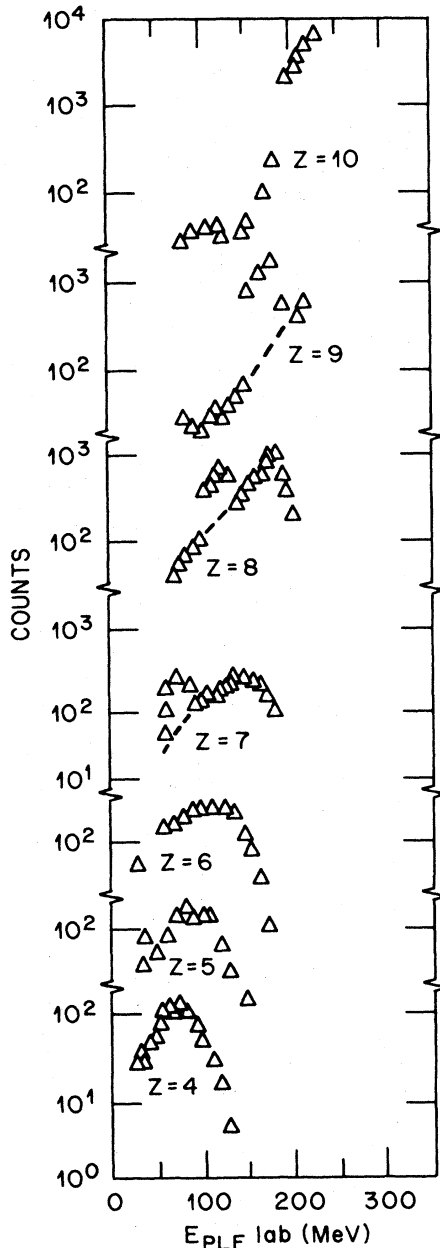


FIG. 2. Laboratory energy distributions of PLF detected in the inner angular range of the position sensitive detector for different elements in the reaction  $^{20}\text{Ne} + ^{150}\text{Nd}$  at 239 MeV. Singles counts for  $Z=7-9$  are contaminated by elastic counts for which no  $\Delta E$  signal was produced. These counts are indicated by the dashed lines.

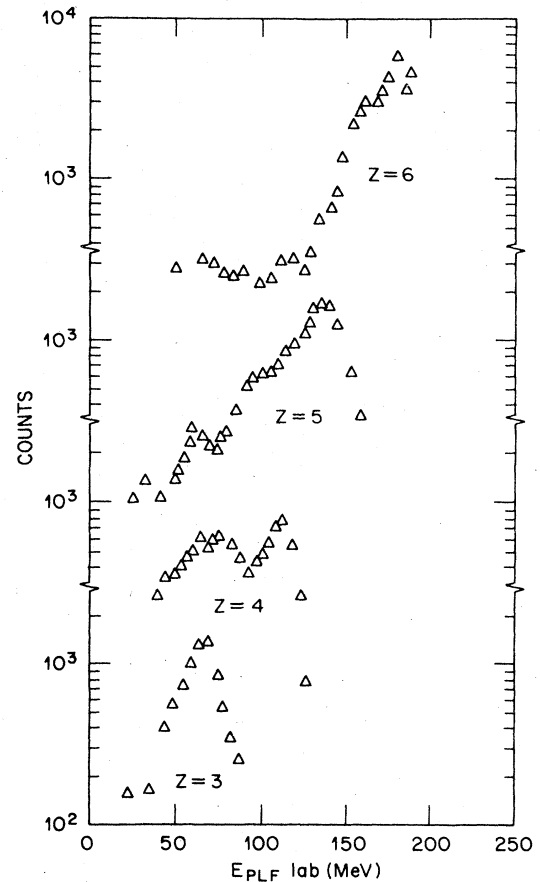


FIG. 3. Laboratory energy distributions of PLF detected in the inner angular range of the position sensitive detector for different charge states in the reaction  $^{12}\text{C} + ^{158}\text{Gd}$  at 192 MeV.

and 18.6 degrees for the C + Gd reaction. The charge distributions of the detected projectilelike fragments are skewed to  $Z$  values smaller than those of the projectiles which seems to be typical for inelastic reactions with light projectiles. The Ne + Nd reaction displayed very similar characteristics at the two energies studied. Neutrons in coincidence with PLF having  $3 \leq Z \leq 6$  for C + Gd and  $4 \leq Z \leq 10$  for Ne + Nd were analyzed in detail. A large number of elastic counts was found to contaminate the  $Z=9$  ridge of the  $\Delta E-E$  spectrum for the Ne + Nd reaction. Because this introduced the possibility of biasing the neutron spectra, events with  $Z=9$  were omitted from the analysis. Energy damping was found to increase with decreasing  $Z$ . This effect was found to be more pronounced for the Ne + Nd reaction where little but quasielastic events are present for  $Z=10$ . By contrast, the energy spectrum of carbon PLF produced in the carbon-induced reaction has a significant deeply inelastic component at laboratory PLF energies below about 125 MeV. We found it convenient for the analysis to express the angular distributions measured using the position sensitive telescope in terms of coefficients  $\alpha(Z)$  such that

$$N/N_0 = 1 - \alpha(Z)(\theta - \theta_0), \quad (1)$$

TABLE II. PLF angular distribution scale factors  $\alpha(Z)$  expressed in units of (degrees) $^{-1}$ .

Z	3	4	5	6	7	8	9	10
C + Gd	0.10	0.15	0.18	0.35 <sup>a</sup>				
Ne + Nd		0.05	0.10	0.18	0.18	0.18	0.30	0.35

<sup>a</sup> Below 125 MeV the correct coefficient is 0.1.

where  $N_0$  is the number of PLF singles having charge  $Z$  detected at the angle  $\theta_0$  which is at the middle of the angular range of the telescope, and  $N$  is the number detected at the angle  $\theta$ . The coefficients  $\alpha(Z)$  for each  $Z$  are shown in Table II. These coefficients were found to be independent of PLF energy except for the case of carbon PLF in the C + Gd reaction. In this case, the angular variation of the quasielastic component was much greater than that of the deeply inelastic component. Therefore, for this case, at energies below 125 MeV the scale factor was found to change from  $\alpha(Z)=0.35$  to 0.1.

The data analysis discussed in Sec. IV, below, relies heavily on the neutron spectra in detector number 6 in coincidence with PLF detected in the inner zone of the position sensitive telescope. No significant differences were found between neutron spectra in coincidence with PLF detected in the inner and outer angular ranges of the telescope except for a decrease in coincidences with increasing angle resulting from the forward peaking of the PLF angular distribution. Therefore, for simplicity and clarity of presentation, the results discussed in the remainder of this paper are for neutrons detected in coincidence with PLF detected over the angular range represented by Figs. 2 and 3; that is, between 19 and 24.6

degrees for the Ne + Nd reaction and between 13 and 18.6 degrees for the C + Gd reaction.

### B. Neutron energy and angular distributions

The neutron emission in the laboratory frame of reference can be described with the Galilean invariant cross section  $d^3\sigma/dV^3$ , where  $\sigma$  is the cross section for neutron emission and  $V$  is the laboratory neutron velocity. Plots are shown in Figs. 4 and 5 of neutron spectra in coincidence with PLF which have the same charge as the projectile for the Ne + Nd reaction at 239 MeV and for the C + Gd reaction, respectively. Contour lines are drawn through the data, each of which represents a doubling of the cross section. A peak in the laboratory neutron spectrum is centered at the angle of detection of the PLF and at the most probable PLF velocity. These figures show that most of the neutrons emitted within the energy and angular range of our detectors were emitted from the fully accelerated PLF. Although this behavior is most apparent for PLF having the projectile charge, similar behavior is seen for neutrons in coincidence with all PLF charge states.

While the cross sections shown in Figs. 4 and 5 show that most of the observed neutrons are associated with the PLF, it remains to be determined whether all of the observed neutrons can be accounted for by assuming that they are emitted from the fully accelerated PLF and TLF or whether it is necessary to assume that some of the neutrons are emitted from some nonequilibrium source.

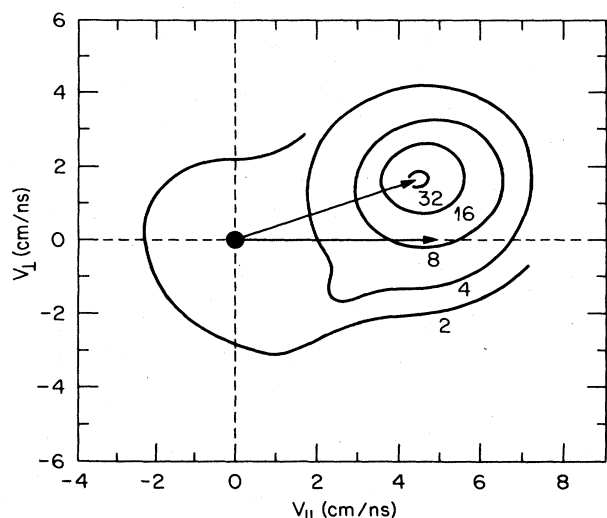


FIG. 4. Contour plot of the Galilean invariant cross section  $d^3\sigma/dV^3$  for neutrons in coincidence with PLF having  $Z=10$  in the reaction Ne + Nd at 239 MeV. One axis is parallel and the other perpendicular to the beam axis. Each contour represents a doubling of the cross section. The arrows at the center represent the beam velocity and most probable PLF velocity. The numbers by each contour are in units of  $10^{-4}$  neutrons/[fragment (cm/ns) $^3$ ].

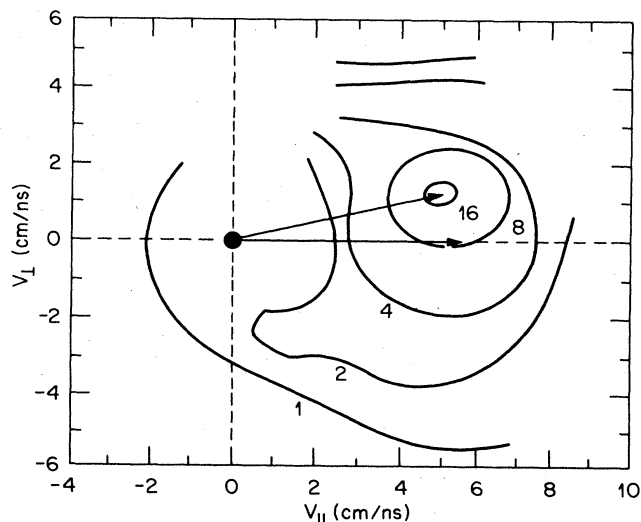


FIG. 5. Same as Fig. 4 but for neutrons in coincidence with PLF having  $Z=6$  in the C + Gd reaction.

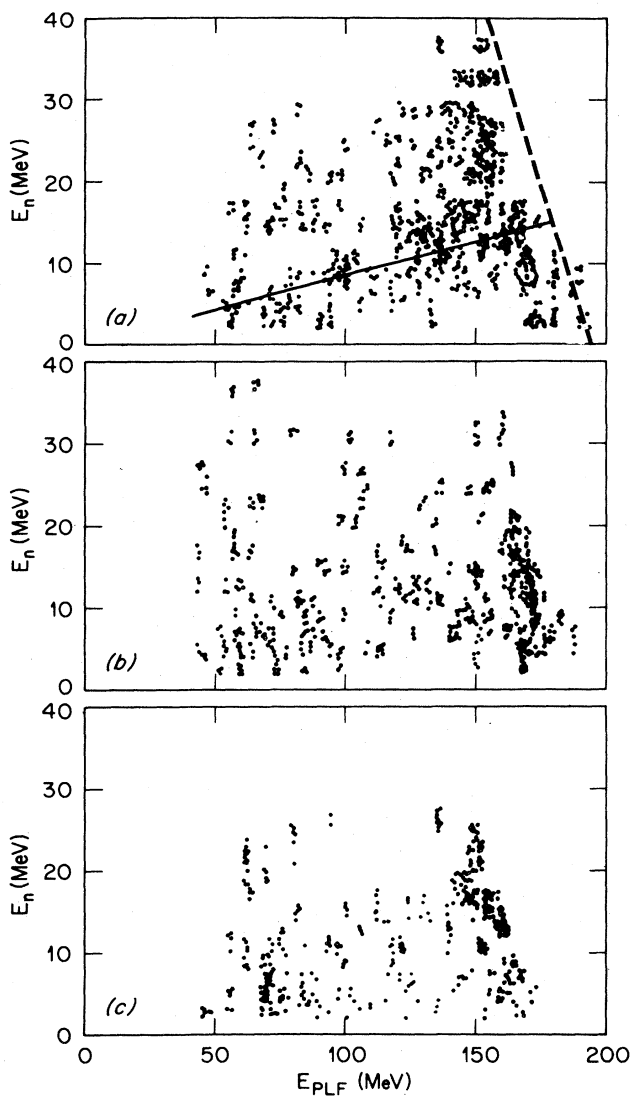


FIG. 6. (a) Neutron counts in detector 6 in coincidence with PLF having the same atomic number as the projectile sorted according to the laboratory energy of the coincident PLF and the laboratory neutron energy. The locus of points for neutrons emitted with zero velocity in the rest frame of the PLF is indicated by the solid line. The dashed line lies on the locus of points for which a neutron is captured and reemitted by the projectile with no excitation of the target or projectile. These data are for the C + Gd reaction. (b) Same as (a) but for neutron counts in detector 5. (c) Same as (b) but for neutrons projected into detector 5.

Further understanding of the emission process may be obtained by displaying a two-dimensional array of PLF energy versus neutron energy (both in the laboratory frame of reference) for each detected element. These are shown in Figs. 6(a) and 7(a) for the C + Gd reaction and the Ne + Nd reaction at 239 MeV. The arrays show neutrons detected by detector number 6, which is at an angle

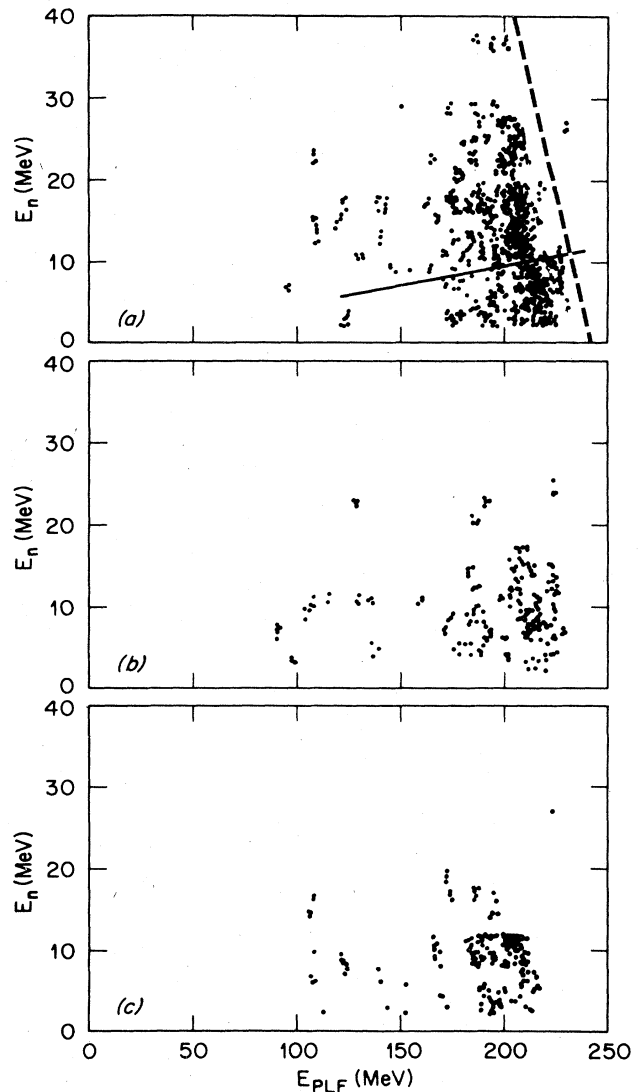
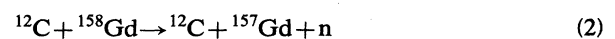


FIG. 7. Same as Fig. 6 but for the Ne + Nd reaction at 239 MeV.

very close to that of the heavy ion telescope in coincidence with PLF having the same atomic number as the projectile. Neutrons emitted from the fully accelerated PLF should be kinematically "focused" into neutron detector 6. Moreover, neutrons emitted toward detector 6 from the fully accelerated PLF with zero velocity relative to the emitting fragment will have laboratory energies equal to the PLF energy per nucleon. The straight lines drawn ascending from left to right across the figures show the locus of points on the  $E_{\text{PLF}}-E_n$  plane for such events, assuming the PLF mass to be twice the PLF charge. The dashed lines in the figures show the locus of points for the reactions



and



with three-body  $Q$  values of  $-7.9$  and  $-7.3$  MeV, respectively. A large number of counts are clustered at these curves, indicating that for both reactions a significant number of events consist of pickup of a neutron from the target with little or no excitation of the target followed by sequential emission of a neutron. The C + Gd data also show evidence of some chance counts at low neutron energy in coincidence with high energy quasielastic PLF, for which the count rate of  $Z = 6$  fragments was very high.

#### IV. ANALYSIS

##### A. Tests for nonequilibrium emission

To test the assumption that all of the observed neutrons are emitted from the fully accelerated fragments in experiments similar to this one, two techniques have commonly been employed. The first approach is to choose as "reference" detectors one back angle detector which observes only neutrons from the TLF and a second one which observes mostly neutrons from the PLF. Spectra for all of the other detectors are then generated by "projecting" the observed neutron counts in these reference detectors into all the other detectors. The projected spectra can then be compared with the observed spectra.<sup>1,2</sup> The second approach is to simulate the experimental data with a computer program based on Monte Carlo techniques. Heavy ion and neutron primary angular and energy distributions are assumed and are used for input. The laboratory neutron spectra produced by the simulation may be compared with the data.<sup>1,6,17</sup> If the energy and angular distributions of the neutron spectra produced by these methods agree with the observed spectra, this can be taken as evidence that the assumption of isotropic emission from fully accelerated fragments is compatible with the experimental data. On the other hand, if there is disagreement, this may provide a basis for estimating the energy and angular distribution of neutrons from some nonequilibrium source or process. The second approach has the advantage that various models for nonequilibrium emission can be included. We have used both techniques to analyze our data and estimate the amount of nonequilibrium neutron emission.

We first used a projection method to test for the presence of nonequilibrium emission. This procedure is discussed in the following paragraphs and the results compared with the neutron spectra recorded in the forward-angle detectors. We then supplemented this with Monte Carlo simulations, to test the sensitivity of the results to various neutron c.m. energy spectra. For the case of the C + Gd reaction we also used Monte Carlo simulations to estimate the nonequilibrium neutron multiplicity.

##### 1. Projections

The projection technique must be applied with great care to experiments with light projectiles, such as the present ones, because of the large recoil effects which distort the angular distribution of neutrons emitted from the PLF. These effects are more severe with alpha emission

measurements<sup>23</sup> but are present in neutron measurements as well.<sup>5,7</sup> The problem arises from the fact that the angular distribution of the PLF varies rapidly at the angle of the heavy ion detector and is forward peaked. This means that there is a greater probability that a PLF, after emitting a neutron, will recoil into the heavy ion detector from an angle forward of this detector than from an angle behind it. This tends to shift the laboratory neutron angular distributions to more forward angles. In the present case this would result in enhanced coincidence rates in neutron detectors 4 and 5 and reduced rates in detectors 6 and 7 compared to the rates that would be expected in the absence of these recoil effects.

The first step in our projection method uses neutron detector number 1 as reference detector for neutrons emitted by the TLF. These counts are projected event by event into all other detectors. That is, for each neutron detected by the reference detector, the neutron energy in the rest frame of the emitting TLF is calculated and then this energy is transformed to the laboratory energies corresponding to emission by the TLF into each of the other detectors. A weighted neutron event is then recorded for each detector at this energy; the assigned weight is proportional to the ratio of the center-of-mass solid angle subtended by the detector into which the count is projected and the angle subtended by the reference detector.<sup>1</sup> The resulting projected spectrum in each of the other detectors can then be subtracted from the observed spectrum and the difference is then assumed to result from neutrons emitted by the fully accelerated PLF and by other possible sources.

Detector number 6 was chosen as the second reference detector because it is at an angle close to that of the PLF detector. Because of kinematic focusing detector 6 will record almost the entire spectrum of neutrons from the PLF. After subtraction of the projected neutron counts from the first reference detector, the spectrum in this detector is itself projected event by event into the other detectors. Provided that this second projection does not put any counts in the first reference detector (detector No. 1), no further iterations are needed and the sum of the two projections can be compared with the data.

The procedure for assigning weights to the projected counts from detector 6 is slightly different from that used for projections of the TLF neutrons because of the need to take into account the recoil effects discussed above. In order to simulate these recoil effects, each neutron is given an additional weight according to whether the emitting PLF recoils from an angle forward of or behind the heavy ion detector. The procedure for doing this was similar to that described in Ref. 24.

We show in Figs. 8–11 the observed neutron energy spectra in the laboratory frame. The projection and simulation procedures indicate that a negligible number of neutrons from the PLF were detected by the back angle detectors. Therefore we present the results for the forward angle detectors only. The results are summed over coincidences for all PLF  $Z$  values. The data (triangles) are shown superimposed on the corresponding projected spectra (dots), together with the results of the Monte Carlo simulations (solid and dashed curves) which are dis-

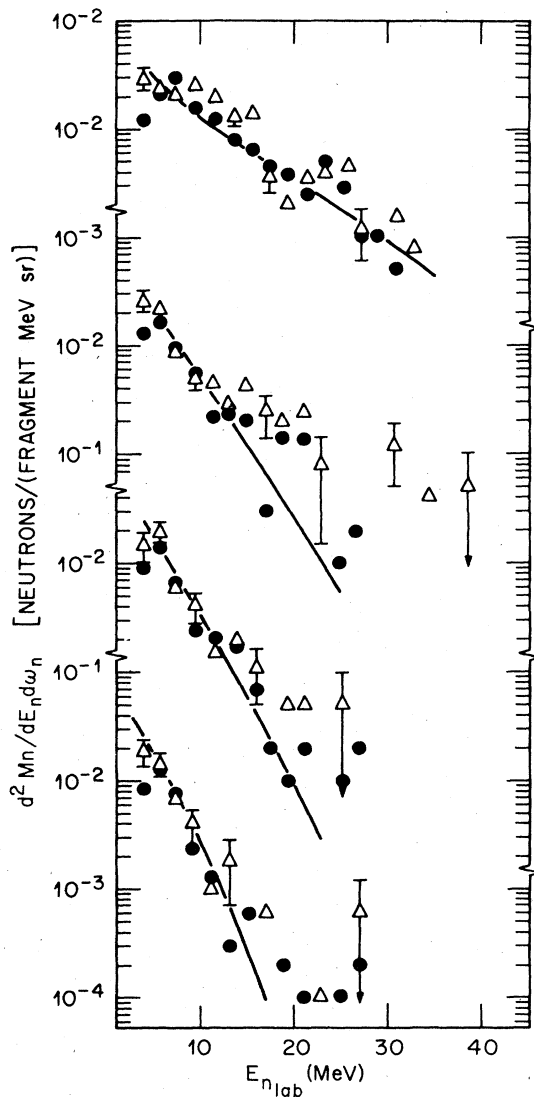


FIG. 8. Observed neutron laboratory energy distributions (triangles), the results of the projection analysis (dots), and Monte Carlo simulations (solid curves) for neutron detectors 2 (bottom) through 5 (top) from the Ne + Nd reaction at 239 MeV. Error bars show only the statistical uncertainty in each point.

cussed in Sec. IV A 2. The spectra for the Ne + Nd reaction in Figs. 8 and 9 show that, within the statistical uncertainty of the experiment, the calculated and observed spectra agree very well. In order to emphasize the agreement between data and projections we show in Fig. 7(b) the data recorded in detector 5 and in Fig. 7(c), for comparison, the projection into the same detector for neutrons in coincidence with PLF having  $Z=10$ . The projections are seen to match the data over the entire  $E_{\text{PLF}}-E_n$  plane. This is true for all detectors and for neutrons in coincidence with all PLF. Thus, based on these projections, we find no evidence for nonequilibrium neutron emission

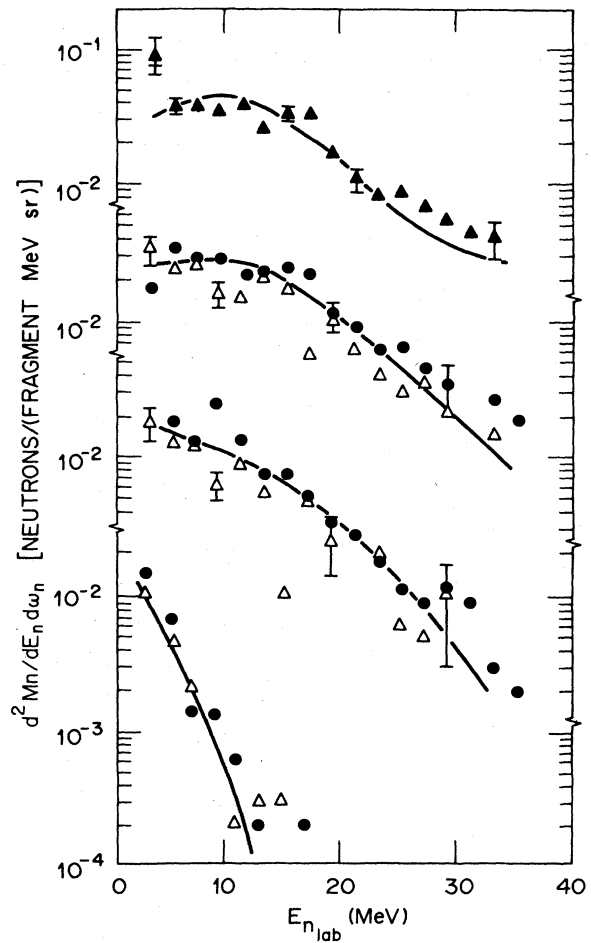


FIG. 9. Same as Fig. 8 but for detectors 6 (top) through 9 (bottom).

in the Ne + Nd reaction at energies up to 239 MeV. Within the sensitivity of our measurements all of the emission can be explained on the basis of isotropic emission from fully accelerated PLF and TLF. These results also indicate that the target remained free from significant contamination by oxygen or carbon during the experiment.

The neutron energy spectra produced in the C + Gd reaction show at high energy a large discrepancy between projections and data in detectors 3, 4, and 5 (Fig. 10) which are the forward angle detectors on the opposite side of the beam from the forward reference detector; above 20 MeV, the measured spectra exceed the projected spectra. For the detectors on the same side of the beam as the forward reference detector (Fig. 11), the data and projections agree very well. Thus, for this reaction, high energy neutrons peaked at forward angles on the opposite side of the beam from the PLF are produced by some mechanism other than by isotropic emission from the PLF. [Similar effects have been observed in the case of the O + Nb reaction at 208 MeV (Ref. 7).] Of course the spectra observed by the reference detector may also include neutrons emit-

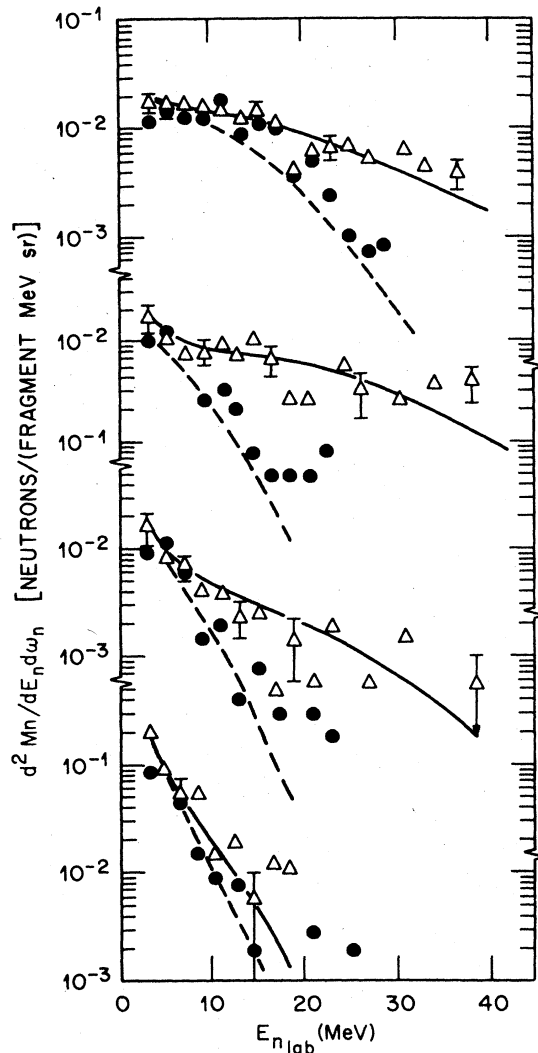


FIG. 10. Neutron laboratory energy distributions (triangles) and projected distributions (dots) for neutron detectors 2 (bottom) through 5 (top) from the C + Gd reaction. Error bars show only the statistical uncertainty in each point. The solid and dashed curves are the results of Monte Carlo simulations described in the text.

ted from a source other than the fully accelerated PLF in such a way that our projection procedure produces a good match between observed and projected spectra on the same side of the beam as the reference detector but not on the opposite side of the beam.

However, contributions to the neutron energy spectra in the forward reference detector from a source different from the fully accelerated PLF cannot completely explain the discrepancy between the measured spectra and the projected spectra on the side of the beam opposite from the reference detector. This is because the angular distribution of high energy neutrons is asymmetric about the beam direction and peaks on the opposite side of the beam from the forward reference neutron detector. This effect

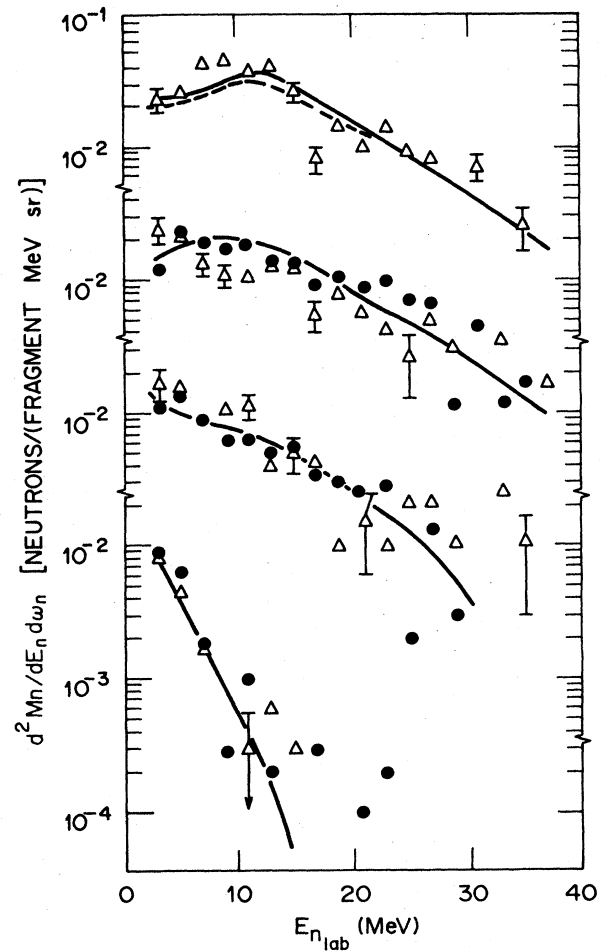


FIG. 11. Same as Fig. 10 but for detectors 6 (top) through 9 (bottom).

is most pronounced for high energy neutrons in coincidence with low energy PLF. It can be seen in Fig. 6 by comparing the number of high energy neutrons in coincidence with low energy PLF on either side of the beam. It is also illustrated in Fig. 12. The two lower curves in this figure show the total number of neutrons with laboratory energies greater than 20 MeV for events in which the three-body  $Q$  value is more negative than  $-70$  MeV (dashed line). One of these curves represents the observed counts and the second, representing the projected counts, is superimposed upon it. The angular distribution of the observed counts is centered at between 10 and 20 degrees from the beam direction on the opposite side of the beam from the heavy ion telescope denoted by the arrow in Fig. 12. The projected counts show an asymmetry about the angle of the telescope due to recoil weighting factors used in the projection but do not show nearly as large an asymmetry as the data. The upper two curves in the figure also show data with projections superimposed but for all  $Q$  values and neutron energies. These two curves also show a discrepancy between data and projections on the opposite side of the beam from the telescope. Although the

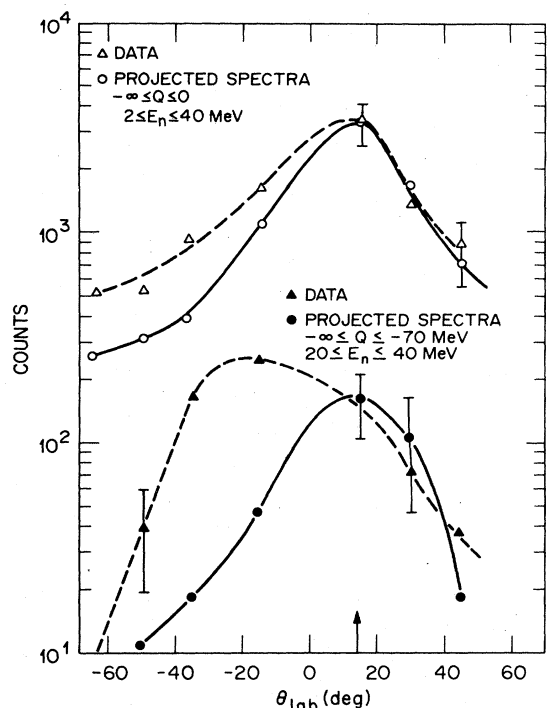


FIG. 12. Total number of neutrons versus laboratory angle. The beam direction is at zero degrees and reference detector 6 is at 15 degrees as indicated by the short vertical arrow. Open triangles denote the distribution for all neutrons with laboratory energies between 2 and 40 MeV. Open circles denote the distribution for all projected neutrons. Closed triangles denote the distribution for neutrons with energies greater than 20 MeV produced in events with two-body  $Q$  value more negative than  $-70$  MeV. Closed circles denote the corresponding projections. Curves are drawn through the points to aid the eye.

difference in counts is greater the percentage difference is smaller than for the lower pair of curves.

## 2. Monte Carlo simulations

To supplement the projection analysis described above and to test the sensitivity of our results to various assumed neutron c.m. energy spectra we also compared the data with the results of a Monte Carlo simulation. Input to this simulation included the measured PLF energy

spectra and angular distributions for all the elements that we have analyzed.

All particle emission was assumed to take place isotropically in the rest frame of the fully accelerated PLF and TLF. The rate of increase of neutron multiplicity with increasing total kinetic energy (TKE) loss was taken from the results of the neutron projection analysis. However, the overall multiplicities of neutrons emitted from both TLF and PLF were treated as independent parameters and were adjusted to give the best agreement with the data. We defer a discussion of these multiplicities to Sec. IV B.

Both the TLF and PLF were assumed to evaporate neutrons with a Boltzmann distribution of the form

$$N(E) = \sqrt{E} \exp(-E/T). \quad (4)$$

The temperature for the TLF and PLF neutron spectra were adjusted independently to give the best fit to the data. In the case of the C + Gd reaction the parameters were adjusted to give the best fit to the spectrum in detectors 6–9 and detectors 1 and 2 where the discrepancies between the observed spectra and the results of the projection analysis are small. The temperature obtained from these fits are shown in Table III.

We show the results of the simulation superimposed on the data points and the projections shown in Figs. 8–11. The results for the Ne + Nd reaction at 239 MeV are shown in Figs. 8 and 9 and we see that the results of the Monte Carlo simulations (smooth curves) do, indeed, agree with the results of the projection analysis and the measured spectra very well. In the case of the C + Gd reaction we expect the simulation to agree with the projection analysis so that the simulated multiplicities will fall well below the measured values in detectors 3–5. The simulated and projected spectra do match very well for all detectors. This is shown by the dashed curves superimposed on the data and projections in Figs. 10 and 11. For detectors 3–5 the simulated multiplicities fall well below the data for large laboratory neutron energies reinforcing the conclusion that nonequilibrium effects are present in this reaction. The solid curves shown in Figs. 10 and 11 are the results of further simulations of the nonequilibrium emission in this reaction. These results are discussed below.

## B. Neutron multiplicities

In order to obtain multiplicity estimates for neutron emission from both PLF and TLF we have first obtained

TABLE III. Temperatures of TLF and PLF and multiplicities of neutrons from PLF and TLF.

Reaction	$T$ (MeV)		Multiplicities		
	$T$ (PLF)	$T$ (TLF)	PLF	TLF	Total
Ne + Nd					
176 MeV	1.5(0.5)	1.5(0.5)	0.14(0.04)	0.8(0.3)	1.0(0.3)
239 MeV	1.5(0.5)	2.0(0.5)	0.30(0.09)	1.9(0.6)	2.2(0.6)
C + Gd	1.5(0.5)	2.0(0.5)	0.4(0.1)	2.2(0.6)	2.6(0.7)

the multiplicity for the PLF as a function of two-body  $Q$  value from the projection analysis. These results are shown in Fig. 13. The solid lines represent least squares straight line fits to the data.

For the Monte Carlo simulations, the overall multiplicities of neutrons from both PLF and TLF were treated as adjustable parameters but the variation with two-body  $Q$  value was taken to be the same for emission from both fragments and was taken from the fits to the data shown in Fig. 13. The multiplicities for PLF determined by the simulations agreed with the values determined from the projection method to within about 10 percent. The largest uncertainty in determining the overall normalization of the neutron multiplicities resulted from the fact that they

were determined from the relatively small number of coincidences obtained during the singles measurements.

The multiplicities deduced from the projection analysis and Monte Carlo simulations and the fragment temperatures deduced from the simulations are shown in Table III. For both systems and at both energies for the Ne + Nd reaction the multiplicities of neutrons from the TLF are found to be approximately six times those of neutrons from the PLF. Moreover, since the temperatures are found to be essentially the same for both fragments in all cases, then the results of the Monte Carlo simulations indicate that the relative amounts of excitation energy removed from the two heavy ion fragments by neutron emission are approximately in the same ratio.

### C. Nonequilibrium emission

Moving source parametrizations for nonequilibrium emission have been used successfully in describing the nonequilibrium emission in coincidence with evaporation residue (ER) in several cases<sup>7-11,18,20,21,25</sup> including our own measurements for the C + Gd and O + Nb systems, although the physical significance of these parametrizations is unclear.<sup>20,21,25</sup> In order to estimate the multiplicity of nonequilibrium neutrons in the C + Gd reaction we have incorporated in our Monte Carlo simulation program a simple *ad hoc* model in which the nonequilibrium neutrons are assumed to be emitted from a moving source.

Because of the asymmetry about the beam axis of our measured nonequilibrium neutron angular distribution, the direction of the moving source was chosen to be within a range of angles centered between the angles of neutron detectors 4 and 5. The distribution of angles for the moving source was a Gaussian. The best results were obtained using a full width at half maximum of 7.5 degrees centered at 22 degrees. The direction was chosen to match the simulated angular distribution to the observed one. The nonequilibrium neutrons were then assumed to be emitted isotropically in the center of mass of this moving source. Within these arbitrary constraints on the direction of travel of the moving source several combinations of source velocity and neutron energy spectra were considered. A combination of source velocity and neutron energy distribution which gives a simulated spectrum matching the data well consists of a source velocity of 0.9 to 1.0 times the beam velocity and a Boltzmann emission spectrum of the form

$$N(E) = E \exp(-E/T).$$

A good match was obtained using a temperature  $T = 2$  MeV and a velocity of 0.9 times the beam velocity. The results are fairly insensitive to this temperature, however, and good results can also be obtained by lowering the temperature and increasing the spread in angle of the PLF or by increasing the temperature and decreasing the source velocity.

The results of this simulation are shown as the solid curves in Figs. 10 and 11. By varying these parameters over the ranges that reproduce the data well we obtain nonequilibrium neutron multiplicities between 0.1 and 0.3, constituting approximately 5 to 14 percent of the total

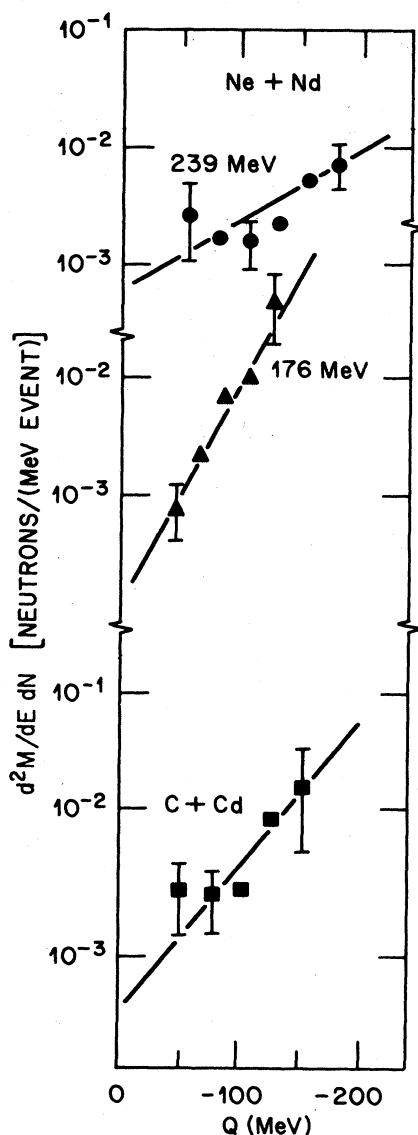


FIG. 13. Multiplicities of observed neutrons as a function of two-body  $Q$  value for neutrons emitted from the PLF. The solid lines are the result of least squares fits to the data.

number of neutrons. This also represents an average energy removal of approximately 3 MeV per event.

Some neutrons from the simulation are observed in detector 6 as shown in Fig. 11. They represent approximately 5% of the total number of neutrons recorded by this detector.

Although the physical significance of this moving source parametrization is unclear it is worthwhile to discuss which models of nonequilibrium emission are consistent with it. First of all, we note that this parametrization is very similar to the ones used by Tserruya *et al.* to describe the nonequilibrium emission in the Kr + Er reaction<sup>8,10</sup> and by Caskey *et al.* for the N + Ho reaction.<sup>12</sup> The parametrization also appears to be consistent with the picture of evaporation with a Maxwellian distribution from a hot moving source.<sup>9,20,25</sup>

The energy distribution of the neutrons is also consistent with a picture of excitation of short-lived states in the composite system that is formed as targetlike and projectilelike fragments orbit about their center of mass. If this is the case then the large source velocity required to reproduce the nonequilibrium neutron energy spectra suggests that the emission takes place from the projectile in the early stages of the reaction before formation of the composite system. (We emphasize that the large source velocity is required to limit the observed nonequilibrium spectra to the narrow range of angles over which they are observed. The observed laboratory energy distribution can be reproduced by lowering the source velocity and increasing the average center-of-mass energy and energy distribution width. However, if this is done, then detectors 6 and 3 show large numbers of nonequilibrium neutrons in the simulation, contrary to the data.)

The spectrum may be consistent with the Fermi-jet or promptly emitted particle (PEP) jet picture of nonequilibrium emission.<sup>26-28</sup> Such a mechanism is expected to produce particles with very large laboratory energies. The calculations published so far using this model have been for neutron emission in coincidence with ER and the angular distributions have consequently all been symmetric about the beam direction. However, it has been noted that diffraction effects are expected to produce angular distributions in coincidence with PLF in inelastic reactions that are asymmetric with respect to the beam direction and peaked on the opposite side of the beam from the detected PLF.<sup>29</sup> Further calculations are needed before we can make any definite conclusions about the applicability of this model to our results.

Our previous conclusion that nonequilibrium emission was present in the C + Gd reaction at lower energies was based on the fact that we were unable, using a Monte Carlo simulation, to reproduce simultaneously both energy spectra and angular distributions of the neutrons from the neutron detectors near in angle to the PLF telescope when we assume that the neutrons were isotropically evaporated from the fully accelerated fragments.<sup>9</sup> By using the projection method of analysis in conjunction with Monte Carlo simulations we have been able in the present case to separate the equilibrium and nonequilibrium components of the neutron spectra and estimate the relative multiplicities of these components. It would, of course, be worthwhile to carry out the same projection scheme on our previous data. This would require, however, an appropriate reference neutron detector directly behind the PLF telescope which we did not have.

In the case of our previous results on nonequilibrium emission associated with evaporation residues the amount of nonequilibrium emission has been found to increase with increasing bombarding energy. Nevertheless no clear-cut threshold has been established for nonequilibrium emission from evaporation residues for either system. We have found that the amount of nonequilibrium emission from the C + Gd system is much larger than from Na + Nd.<sup>20</sup> The results of the present experiment indicate that the same situation holds for emission from products of inelastic reactions from these two systems.

## V. CONCLUSIONS

In the present paper we report on neutron emission in coincidence with products of inelastic scattering reactions in the systems C + Gd at 192 MeV and Ne + Nd at 176 and 239 MeV bombarding energies. We have found evidence for a small amount (approximately 9% of the total number of neutrons emitted) of nonequilibrium neutron emission in the C + Gd reaction; we find no evidence for nonequilibrium emission in the Ne + Nd reaction at either energy. Instead, all neutron emission in this system can be accounted for on the basis of sequential emission from the fully accelerated PLF and TLF.

This work was supported by the Office of High Energy and Nuclear Physics of the United States Department of Energy.

\*Present address: Institut de Physique Nucleaire de Lyon, Villeurbanne, France.

<sup>1</sup>Y. Eyal, A. Gavron, I. Tserruya, Z. Fraenkel, Y. Eisen, S. Wald, R. Bass, C. R. Gould, G. Kreyling, R. Renfordt, K. Stelzer, R. Zitzmann, A. Gobbi, A. Lynen, H. Stelzer, I. Rode, and R. Bock, *Phys. Rev. Lett.* **41**, 625 (1978).

<sup>2</sup>D. Hilscher, J. R. Birkelund, A. D. Hoover, W. U. Schroder, W. W. Wilcke, J. R. Huizenga, A. C. Mignerey, K. L. Wolf, H. F. Breuer, and V. E. Viola, Jr., *Phys. Rev. C* **20**, 576 (1979).

<sup>3</sup>B. Tamain, R. Chechik, H. Fuchs, F. Hanappe, M. Morjean, C. Ngo, J. Peter, M. Dakowski, B. Lucas, C. Mazur, M. Ribrag, and C. Signarbieux, *Nucl. Phys.* **A330**, 253 (1979).

<sup>4</sup>C. R. Gould, R. Bass, J. v. Czarnecki, V. Hartmann, K. Stelzer, R. Zitzmann, and Y. Eyal, *Z. Phys. A* **294**, 323 (1980).

<sup>5</sup>S. Wald, I. Tserruya, Z. Fraenkel, G. Doukellis, H. Gemmeke, and H. L. Harney, *Phys. Rev. C* **28**, 1538 (1983).

<sup>6</sup>H. Gemmeke, P. Netter, A. Richter, L. Lassen, S. Lewandowski, W. Lucking, and R. Schreck, *Phys. Lett.* **B97**, 213

- (1980).
- <sup>7</sup>A. Gavron, R. L. Ferguson, Felix E. Obenshain, F. Plasil, G. R. Young, G. A. Petitt, K. Geoffroy Young, D. G. Sarantites, and C. F. Maguire, *Phys. Rev. Lett.* **46**, 8 (1981).
- <sup>8</sup>I. Tserruya, A. Breskin, R. Chechik, Z. Fraenkel, S. Wald, N. Zwang, R. Bock, M. Dakowski, A. Gobbi, H. Sann, R. Bass, G. Kreyling, R. Renfordt, K. Stelzer, and U. Arlt, *Phys. Rev. Lett.* **47**, 16 (1981).
- <sup>9</sup>A. Gavron, J. R. Beene, R. L. Ferguson, F. E. Obenshain, F. Plasil, G. R. Young, G. A. Petitt, K. Geoffroy Young, M. Jaaskelainen, D. G. Sarantites, and C. F. Maguire, *Phys. Rev. C* **24**, 2048 (1981).
- <sup>10</sup>I. Tserruya, A. Breskin, R. Chechik, Z. Fraenkel, S. Wald, N. Zwang, R. Bock, M. Dakowski, A. Gobbi, H. Sann, R. Bass, G. Kreyling, R. Renfordt, K. Stelzer, and U. Arlt, *Phys. Rev. C* **26**, 2509 (1982).
- <sup>11</sup>D. Hilscher, E. Holub, G. Ingold, U. Jahnke, H. Orf, H. Rossner, W. U. Schroder, H. Gemmeke, K. Keller, L. Lassen, and W. Lucking, *Proceedings of the Workshop on Coincidence Particle Emission from Continuum States*, Bad Honnef, 1984.
- <sup>12</sup>G. Caskey, A. Galonsky, B. Remington, M. B. Tsang, C. K. Gelbke, A. Kiss, F. Deak, Z. Seres, J. J. Kolata, J. Hinnefeld, and J. Kasagi, *Phys. Rev. C* **31**, 1597 (1985).
- <sup>13</sup>D. L. Hillis, O. Christensen, B. Fernandez, A. J. Ferguson, J. D. Garrett, G. B. Hagemann, B. Herskind, B. B. Back, and F. Folkmann, *Phys. Lett.* **B78**, 405 (1978).
- <sup>14</sup>L. Westerberg, D. G. Sarantites, D. C. Hensley, R. A. Dayras, M. L. Halbert, and J. H. Barker, *Phys. Rev. C* **18**, 796 (1978).
- <sup>15</sup>J. R. Beene, M. L. Halbert, D. C. Hensley, R. A. Dayras, K. Geoffroy Young, D. G. Sarantites, and J. H. Barker, *Phys. Rev. C* **23**, 2463 (1981).
- <sup>16</sup>K. Geoffroy Young, D. G. Sarantites, J. R. Beene, M. L. Halbert, D. C. Hensley, R. A. Dayras, and J. H. Barker, *Phys. Rev. C* **23**, 2479 (1981).
- <sup>17</sup>J. Kasagi, S. Saini, T. C. Awes, A. Galonsky, C. K. Gelbke, G. Poggi, D. K. Scott, K. L. Wolf, and R. L. Legrain, *Phys. Lett.* **B104**, 434 (1981).
- <sup>18</sup>D. Hilscher, E. Holub, U. Jahnke, H. Orf, and H. Rossner, in *Dynamics of Heavy Ion Collisions, Proceedings of the Third Adriatic Europhysics Study Conference, Hvar, Yugoslavia, 1981*, edited by N. Cindro, R. A. Ricci, and W. Greinen (North-Holland, Amsterdam, 1981), p. 225.
- <sup>19</sup>A. Gavron, J. R. Beene, B. Cheynis, R. L. Ferguson, F. E. Obenshain, F. Plasil, G. R. Young, G. A. Petitt, M. Jaaskelainen, D. G. Sarantites, and C. F. Maguire, *Phys. Rev. Lett.* **47**, 1255 (1981); **48**, 835(E) (1982).
- <sup>20</sup>A. Gavron, J. R. Beene, B. Cheynis, R. L. Ferguson, F. E. Obenshain, F. Plasil, G. R. Young, G. A. Petitt, C. F. Maguire, D. G. Sarantites, M. Jaaskelainen, and K. Geoffroy Young, *Phys. Rev. C* **27**, 450 (1983).
- <sup>21</sup>E. Holub, D. Hilscher, G. Ingold, U. Jahnke, H. Orf, and H. Rossner, *Phys. Rev. C* **28**, 252 (1983).
- <sup>22</sup>M. Drog, *Nucl. Instrum. Methods* **105**, 573 (1972).
- <sup>23</sup>G. R. Young, R. L. Ferguson, A. Gavron, D. C. Hensley, F. E. Obenshain, F. Plasil, A. H. Snell, M. P. Webb, C. F. Maguire, and G. A. Petitt, *Phys. Rev. Lett.* **45**, 1389 (1980).
- <sup>24</sup>S. Wald, Z. Fraenkel, and I. Tserruya, *Nucl. Instrum. Methods* **206**, 119 (1983).
- <sup>25</sup>T. C. Awes, G. Poggi, C. K. Gelbke, B. B. Back, B. G. Glagola, H. Breuer, and V. E. Viola, Jr., *Phys. Rev. C* **24**, 89 (1981).
- <sup>26</sup>J. P. Bondorf, J. N. De, A. O. T. Karvinen, G. Fai, and B. Jakobsson, *Phys. Lett.* **B84**, 162 (1979).
- <sup>27</sup>W. J. Swiatecki, Lawrence Berkeley Laboratory Report No. LBL-8590, 1979.
- <sup>28</sup>J. P. Bondorf, J. N. De, G. Fai, A. O. T. Karvinen, B. Jakobsson, and J. Randrup, *Nucl. Phys.* **A333**, 285 (1980).
- <sup>29</sup>A. S. Umar, M. R. Strayer, and D. J. Ernst, *Phys. Rev.* **140B**, 290 (1984).